processes

MDPI

Article

Enhancing Thermal Performance of Vertical Ground Heat Exchangers Through a Central Borehole Removal Design

Ahmad Aljabr

Department of Mechanical and Industrial Engineering, College of Engineering, Majmaah University, Al-Majmaah 11952, Saudi Arabia; aa.aljabr@mu.edu.sa

Abstract: The high initial cost of ground heat exchanger (GHE) systems, particularly in applications with significant annual building thermal load imbalances, remains a major barrier to their adoption. In traditional rectangular grid patterns of boreholes, thermal saturation in cooling-dominated buildings mainly affects the central zone, rendering central boreholes less effective. This study investigates an innovative approach to enhance the thermal performance of vertical GHEs by removing these central boreholes using the pygfunction Python package. The central borehole removal design (CBRD) was implemented across various building thermal loads and ground conditions, resulting in reduced borehole interaction and a substantial decrease in total GHE length. Specifically, the CBRD approach achieved up to 51% savings in total GHE length compared to traditional rectangular grid patterns, significantly lowering the initial cost without additional expenses. Although energy consumption savings over a 30-year period were modest (up to 2.2%), the initial cost savings were substantial. Further optimizations indicated that additional reductions in borehole length could be achieved by removing boreholes beyond the central ones, while still maintaining the maximum entering fluid temperature (EFT). Yet, additional optimizations are needed as achieving optimal configurations requires detailed information on factors such as available land area and drilling depth limits, which are site-specific.

Keywords: central boreholes removal design; vertical ground heat exchanger; pygfunction Python package; geothermal energy; innovative borehole layout



Academic Editor: Sergey Y. Yurish

Received: 22 December 2024
Revised: 20 January 2025
Accepted: 21 January 2025
Published: 25 January 2025

Citation: Aljabr, A. Enhancing Thermal Performance of Vertical Ground Heat Exchangers Through a Central Borehole Removal Design. *Processes* **2025**, *13*, 333. https://doi.org/10.3390/pr13020333

Copyright: © 2025 by the author. Licensee MDPI, Basel, Switzerland. This article is an open access article distributed under the terms and conditions of the Creative Commons Attribution (CC BY) license (https://creativecommons.org/licenses/by/4.0/).

1. Introduction

Renewable energy systems play a crucial role in meeting the high cooling and heating demands of buildings by offering sustainable and efficient alternatives to traditional energy sources [1,2]. Technologies like geothermal systems utilize the Earth's stable temperature to heat and cool spaces [3,4]. These systems not only reduce carbon emissions but also offer long-term cost savings and resilience against fluctuating energy prices. Ground heat exchangers (GHEs) are a common component in geothermal heat pump systems, providing efficient heating and cooling solutions by exchanging heat with the ground [5]. GHE setups typically involve transferring heat between a liquid moving through a closed circuit buried underground and the surrounding soil. They are available in distinctive designs, such as horizontal [6] and vertical configurations, closed-circuit and open-circuit arrangements, and have become increasingly popular as eco-friendly options for climate control in homes, offices, and factories [7].

Despite their potential, the high capital cost of GHE systems remains a significant barrier to their widespread adoption. This challenge is especially pronounced in applications with substantial annual load imbalances, where the heat rejected into the ground

during cooling seasons substantially exceeds the heat extracted during heating seasons, or vice versa. These imbalances can cause thermal saturation of the ground, diminishing the system's overall performance and efficiency [8]. The heat transfer from the borehole to the surrounding ground is usually described by g-function profiles. g-function profiles represent the thermal response of a borehole field to a unit heat input over time, and they play a crucial role in calculating the thermal interaction between boreholes. By analyzing g-function profiles, it is possible to understand how the arrangement of boreholes and the ground's thermal properties influence the overall performance and efficiency of the GHE system.

The prevalence and significance of cooling-dominated buildings in ground-source heat pump (GSHP) system design have been well recognized in the literature [9]. For example, Li et al. [10] investigated how soil thermal imbalance affects the efficiency of GSHP systems. Their findings revealed a strong correlation between the thermal imbalance ratio of cumulative building loads and system performance. Specifically, as the imbalance ratio increased, they observed a substantial rise in the GHE outlet water temperature, amounting to 10.7 °C. This temperature increase had a dramatic impact on the system's cooling coefficient of performance (COP), reducing it by approximately 50%. These results underscore the critical importance of addressing thermal imbalance in GSHP system design and operation. Similarly, Chen et al. [11] demonstrated that ignoring GHE interconnections can significantly overestimate thermal imbalance, particularly under varying load conditions. They suggested a self-adjusting mechanism that maintains the thermal balance of the borehole field.

The depth of boreholes directly impacts the effectiveness of heat exchange between the circulating fluid and the underground layers, making this factor crucial in the design and installation of geothermal systems [12]. Numerous strategies have been proposed in the literature to reduce the capital cost of GHE systems. Enhancements such as improving the thermal conductivity of pipe materials [13], using alternative refrigerants [14], and integrating phase change materials with the grout have shown promise [15]. Additionally, the inclusion of supplemental heat rejection or absorption components can help manage ground load more effectively, offsetting some of the thermal imbalance [16]. For example, air-source heat compensators [17] and heat compensation units with thermosyphons [18] have been suggested for combination with GSHP systems to compensate for heat into the ground. While these methods can improve system performance and reduce operational costs, they often introduce additional complexities and expenses, thereby not fully addressing the issue of high initial investment [19].

Moreover, the conventional approach to designing borehole fields typically adheres to a rectangular grid pattern, constrained by the limitations of existing design tools. Current commercial tools used for vertical GHEs typically employ pre-calculated response functions called g-functions [20]. These tools often restrict the exploration of unconventional designs, such as a central borehole removal design (CBRD) [21]. The Eskilson g-function is widely used but is limited to specific geometries and field layouts [22]. However, nontraditional GHE designs, such as those involving borehole removal and varying spacing, have gained attention as they offer potential cost savings and efficiency improvements by addressing thermal saturation more effectively than conventional layouts. To address these constraints, researchers have developed alternative forms of g-functions. Recently, new tools such as the Chiasson GHX Toolbox [23] and the Python package pygfunction [24] have emerged, allowing for more flexible and innovative borehole field configurations. Cimmino and Bernier [25] segmented boreholes to account for heat transfer rates across their depths. Cimmino later refined this approach [26] and released it as the Python package pygfunc-

tion [24]. These tools enable the exploration of nontraditional borehole patterns, offering potential pathways to enhance the efficiency of GHE systems.

One example of such nontraditional borehole field patterns includes zoned subfields with on-off control [27]. In this configuration, the GHE field is split into two zones to reduce thermal concentration at the center. Zone 1 manages the fundamental loads and remains active continuously, while Zone 2 operates when the GHE fluid temperature approaches within 2.7 °C of the maximum or minimum design temperatures. The findings indicate that zoning the borehole field can significantly decrease the size of the field in situations with predominant loads. Bayer et al. [28] noted that by removing less effective boreholes typically located at the center, where thermal saturation can occur, both the quantity and total length of boreholes can be reduced, resulting in consistent heat transfer across the entire field. Another example is varying borehole spacing [29], which involves widening the gaps within the central area of the field while narrowing them around the edges. This strategy resulted in savings ranging from 6% to 15% compared to a standard rectangular arrangement with uniform spacing. Wrap-around configurations, where boreholes are positioned encircling the structure, were also investigated [29]. This configuration led to a reduction in total drilling depth by 34% to 42.6% compared to a rectangular configuration on one side of the building. Designing mixed borehole depths within the same field is another innovative approach [30]. In this design, shorter boreholes are placed in the central area and deeper ones around the perimeter. Findings showed that in certain scenarios of mixed borehole depths, the total length of borehole heat exchangers (BHEs) could be reduced by as much as 10% compared to configurations with uniform borehole depths. These innovative designs improve thermal interaction between the boreholes and the surrounding ground, mitigating thermal saturation and enhancing overall system performance with insignificant extra cost.

To the best of the author's knowledge, limited research exists on the design approach involving the removal of central boreholes, as illustrated in Figure 1. Although some studies have explored variations in borehole field patterns, few have specifically investigated the strategic removal of central boreholes to improve thermal performance. The goal of this paper is to propose and evaluate a novel design approach for GHE systems by removing central boreholes, aiming to improve thermal performance and reduce costs. The approach presented here builds on recent advancements in flexible simulation tools and nontraditional borehole configurations but introduces a more direct and practical solution for managing ground thermal saturation. The central region of a borehole field typically experiences thermal saturation most rapidly due to the cumulative effect of heat exchange from surrounding boreholes, especially with the traditional rectangular grid patterns for boreholes. By strategically removing some of these central boreholes, it is possible to enhance the thermal performance of the system, potentially reducing costs and improving efficiency. The proposed design approach will be examined in different climate zones and subsurface geologies to generalize the potential savings in various scenarios. This investigation is conducted using the validated Python package pygfunction version 2.2 [31], which has been adapted in this paper to achieve this goal.

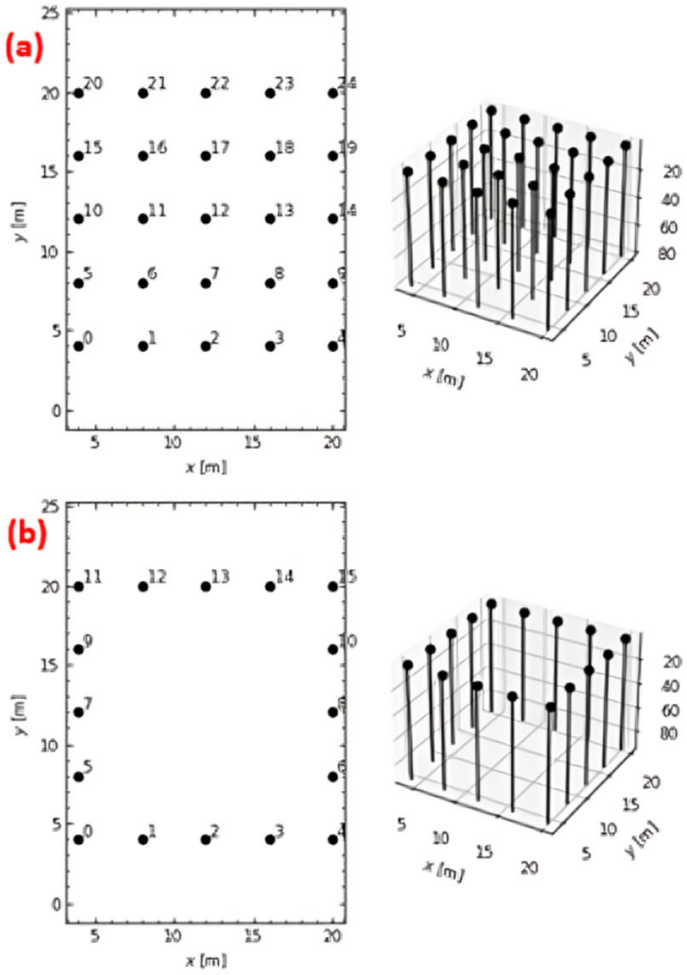


Figure 1. Bore field layout at (**a**) traditional layout design, and (**b**) central boreholes removal design.

2. Methodology

Simulating the GHE's performance entails calculating the hourly outlet fluid temperature and the heat pump energy consumption. This study utilizes a simulation approach based on a temperature response factor known as the g-function, generated using the pygfunction Python package [31]. A flowchart of the GHE simulation process, shown in Figure 2, provides an overview of the key steps involved in the simulation using the pygfunction package. A comprehensive explanation of the computation process using the pygfunction code is detailed in [26], and this paper mainly utilizes the same code, thus avoiding redundancy in its description. One limitation of the proposed method is that it does not account for potential changes in flow direction within the bore field over time, which may occur in certain seasonal storage systems. The pygfunction software enables unconventional designs for bore fields, such as arbitrary borehole positioning, and has been customized in this study to accept file-based inputs for borehole characteristics. Within this input file, each borehole in the field is defined by five primary attributes: its coordinates in both the x and y directions, its total depth, the depth at which it is buried, and its radius. The simulation procedure for GHE involves three main stages: First, specifying the characteristics of the bore field (including borehole count, properties, spacing, and ground thermal and physical attributes); Second, generating the corresponding g-function for the bore field; and third, integrating the building's hourly thermal loads to compute the heat exchange with the ground.

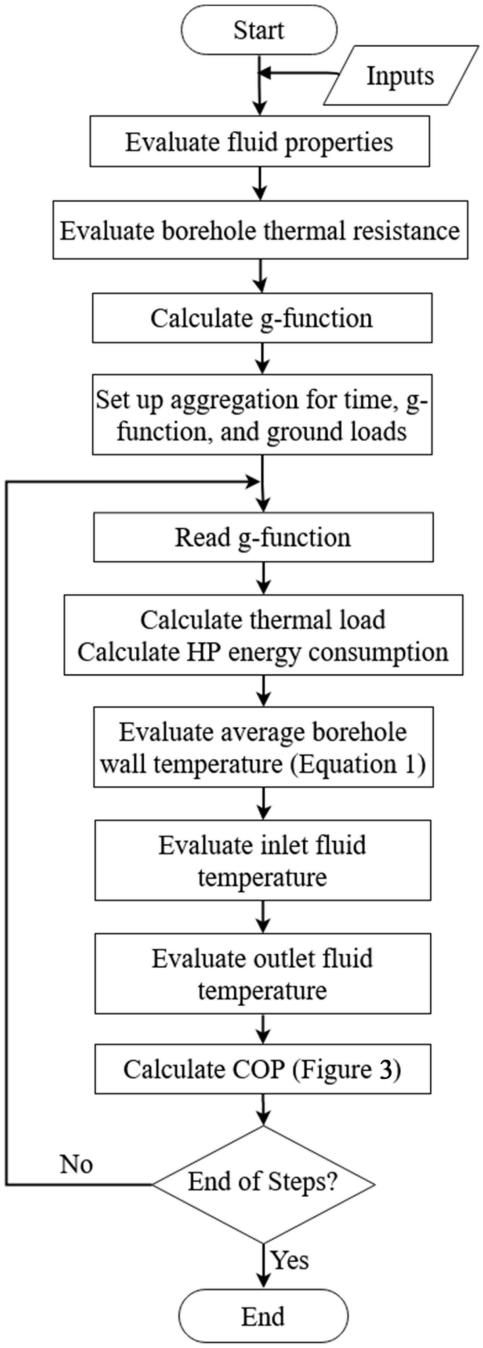


Figure 2. Flowchart of the GHE simulation in pygfunction.

2.1. Borehole Field

The pygfunction code has been adjusted to read the main characteristics of each borehole in the field from a text file, including their x- and y-coordinate positions, depths, buried depths, and radii. Each borehole is uniquely identified and linked with its specific attributes. Additional parameters defining the borehole field are specified within the main code file, as detailed in Table 1. Thermal resistance in boreholes is computed using the multipole method introduced by Claesson and Hellstrom [32], which considers the thermal resistance contributions from components such as the pipe, fluid, and grout. The generated g-function incorporates the short-term effects influenced by the borehole's thermal resistance under transient conditions within the borehole. The fluid used is propylene-glycol (20%) with a steady mass flow rate of 0.073 kg s^{-1}.

Table 1. Specifications of the GHE field [31].

Component	Specification	Value
Ground	Ground thermal conductivity	Based on location
	Ground thermal diffusivity	1.14×10^{-6} m^2 s^{-1}
	Undisturbed ground temperature	Based on location
Borehole	Borehole radius	0.075 m
	Grout thermal conductivity	1.5 W m^{-1} K^{-1}
	Borehole buried depth	1.0 m
	Boreholes connection	parallel
	Boreholes spacing	4.0 m
Pipe (HDPE)	Pipe outer radius	0.01335 m
	Pipe inner radius	0.0109 m
	half the distance between pipe centers	0.06115 m
	Pipe configuration (single U-tube)	evenly spaced
	Pipe thermal conductivity	0.4 W m^{-1} K^{-1}

Initially, it is assumed that the ground is homogeneous and isotropic (the soil has uniform thermal properties, such as thermal conductivity, in all directions), maintaining a uniform temperature (the ground is at a steady state and has no significant variations in temperature across the borehole field), with no groundwater flow, so the heat transfer within the ground is solely through conduction. While the performance of GSHP systems can be influenced by groundwater flow, this study does not account for groundwater effects due to limited detailed data on groundwater flow characteristics (flow rate, direction, and depth) for all examined locations, particularly between coastal and inland cities. In the design of a GSHP system for a specific site, an in situ test, typically a thermal response test (TRT) is often conducted. This test measures thermal properties such as thermal conductivity and initial ground temperature across different soil layers to provide more accurate data, including insights into groundwater presence.

2.2. GSHP Simulation

Simulating the GHE's performance entails calculating the hourly entering fluid temperature (EFT) and the heat pump energy consumption. Figure 2 provides an illustration of the simulation procedure in pygfunction. In this study, a simulation time-step of one hour over 30 years ensures that the GHE approaches a steady state. The simulation in pygfunction starts with reading the borehole and ground characteristics as detailed in the Borehole Field subsection and Table 1, along with ground thermal loads specified in the Case Studies subsection. The fluid properties are evaluated at 20 °C before calculating the borehole thermal resistance.

The long-term g-function is defined by four ratios: $\mathrm{g}\left(\frac{r_b}{H}, \frac{B}{H}, \frac{D}{H}, \frac{t}{t_s}\right)$, where r_b, B, D, and H are the borehole's radius, spacing, buried depth, and depth, respectively. The last ratio represents the ratio of time to the steady-state time of the field ($t_s = H^2/9\alpha_s$). This Eskilson long-term g-function appears in the general solution of the BHE heat transfer problem [23]:

$$T_b = T_g - \frac{Q\prime}{2\pi k_s} \cdot \mathrm{g}\left(\frac{r_b}{H}, \frac{B}{H}, \frac{D}{H}, \frac{t}{t_s}\right) \quad (1)$$

This formula determines the borehole wall temperature (T_b) using the undisturbed ground temperature (T_g) and the average heat exchange rate per borehole length (Q'). The finite line source solution in Equation (1) is implemented by dividing each borehole into eight finite line source segments [25], assuming a uniform inlet fluid temperature (inlet fluid temperature is the same for each borehole in the field).

To manage the computational demand, pygfunction incorporates an aggregation algorithm developed by Claesson and Javed [33], which reduces the simulation time. This approach is logical, as more recent ground thermal loads have a greater impact than older ones [23]. The pygfunction has been modified to read hourly ground thermal loads from a text file. Both the ground thermal load and the g-function are updated at each time step due to the dynamic nature of ground thermal load and storage.

For every time interval, the simulation process applies the ground thermal load to determine the average temperature along the depth of each borehole's wall (Equation (1)). This temperature is then used to calculate the inlet fluid temperature [26], which remains constant across all boreholes. Subsequently, the EFT is computed for each time step [26].

The heat pump's operational characteristics are detailed in Figure 3, varying with the EFT for both heating and cooling modes. This model of a typical heat pump assumes a linear relationship between EFT and the COP. Notably, the pygfunction code does not incorporate fluid circulation pumping energy or account for energy losses.

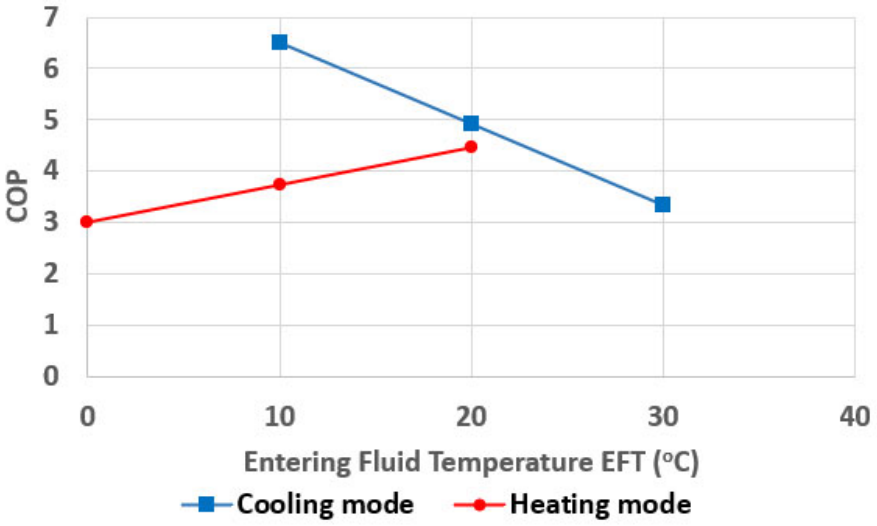


Figure 3. Typical COPs of the ground source heat pump.

2.3. Case Studies

The design and performance of vertical borehole heat exchangers are significantly influenced by both the climate type and the geological conditions beneath the surface. Because the proposed design approach will be examined in different climate zones and subsurface geologies to generalize the potential savings in various scenarios, Saudi Arabia, which has six climate zones and various subsurface geologies, is chosen as a case study. The six locations chosen in this study correspond to six of the seven locations studied in [34]: Riyadh for the hot-dry desert subzone, Jeddah for the hot-dry maritime desert subzone, Dhahran for the hot-dry maritime subzone, Tabuk and Turaif for the cold-dry desert subzone, and Jizan for the hot-dry maritime desert subzone. The last climate zone (subtropical with a Mediterranean subzone and a mountainous subtype represented by Abha in [34]) is excluded here because it requires only three boreholes to meet the building thermal load, which is inapplicable for the approach of central borehole removal design. Table 2 details the annual average air temperature in each city [34]. The ground

characteristics of the six locations—including undisturbed ground temperature and ground thermal conductivity—are specified from the previous work [34] and are shown in Table 2. These six locations represent a wide range of climate zones and ground properties.

Table 2. The average air temperature, ground properties, and peak loads of each site [34].

Description	Riyadh	Jeddah	Dhahran	Tabuk	Jizan	Turaif
Average air temperature (°C)	25.7	28.2	26.5	21.9	30.2	18.9
Undisturbed ground temperature (°C)	25.7	28.2	26.5	21.9	30.2	18.9
Ground thermal conductivity (W m^{-1} K^{-1})	2.63	1.70	2.15	2.80	1.70	2.80
Peak cooling (kW)	29.6	29.6	31.4	30.0	26.8	29
Peak heating (kW)	9.9	0.6	7.5	11.2	0.0	15
Cooling/Heating peak ratio	3.0	49.3	4.2	2.7	-	1.9

In this study, a simulation time-step of one hour over 30 years ensures that the GHE approaches a steady state. Therefore, hourly building thermal loads are integrated into the model. The hourly building thermal loads used in [34], validated with [35], are used here and summarized in Table 2 and Figure 4. All locations feature primarily cooling-dominated buildings, experiencing a significant imbalance between annual heating and cooling thermal loads, which is expected in Saudi Arabia's residential buildings [36]. Specifically, the cooling peak load is at least twice the heating peak load. Therefore, the ground temperature is expected to increase over the lifetime of the GSHP system in all selected locations.

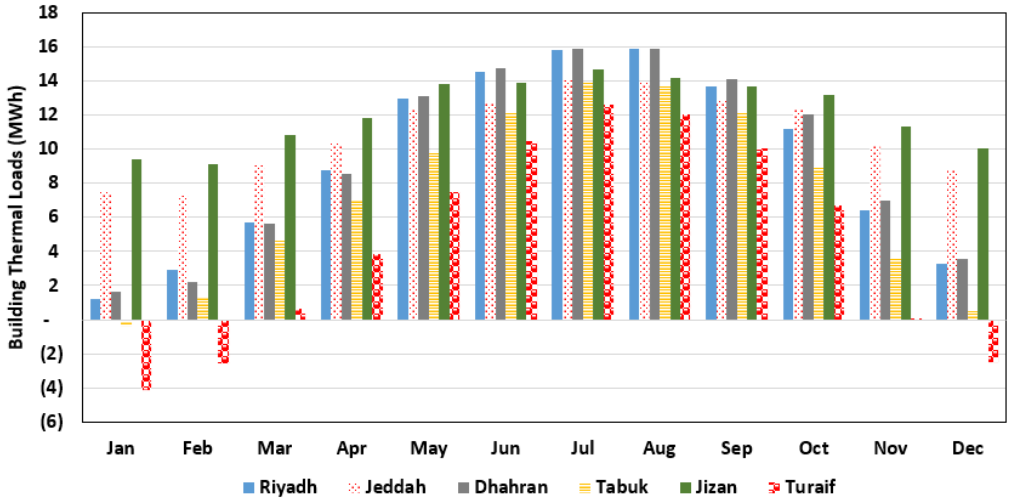


Figure 4. Building thermal loads.

Another reason for choosing locations in Saudi Arabia is that a typical house is centrally built on the land, leaving open spaces around the building, as illustrated in Figure 5. The layout is typical of many residential designs in the region, which often prioritize maintaining open spaces around buildings for privacy, ventilation, and aesthetic reasons. This common layout is highly conducive to the central borehole removal design approach presented in this study. Each house is required to maintain a specific setback (horizontal distance between the building's outer wall and the land border) of at least two meters on all four sides [37].

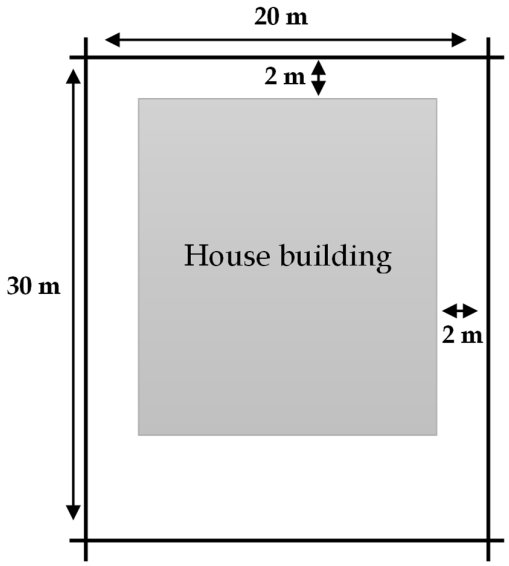


Figure 5. Typical layout of house buildings in Saudi Arabia [37].

3. Results and Discussion

Firstly, the study establishes baseline outcomes for a GHE system using a traditional borehole layout as reference cases. Subsequently, the investigation explores the adoption of the proposed strategy involving the removal of central boreholes from the grid, examining various thermal loads and ground conditions. The primary objective of this investigation is to assess how the elimination of central boreholes affects the thermal efficiency of GHE systems and its potential for economical implementation in environments with imbalanced thermal loads. The results are evaluated based on key performance metrics, including thermal efficiency, ground temperature variation, and total initial cost. Furthermore, the discussion explores the implications of central borehole removal on the operational efficiency and economic feasibility of GHE systems.

Because of the building's emphasis on cooling and its significant disparity between heating and cooling thermal loads over the year, the reference GHE system is designed to maintain a maximum EFT of 40 °C throughout its 30-year operational period. Given that the pygfunction code currently lacks an optimization feature, the simulation process is performed iteratively for each location to optimize the total length of the GHE and ensure it meets the maximum EFT criteria.

3.1. Reference Cases

Figure 6 shows the results of the GHE simulations across all cases, with detailed data provided in Table 3. In the reference cases, borehole depth and spacing are consistent across all locations (80 m and 4 m, respectively), while the number of boreholes varies depending on building thermal loads and ground conditions. Specifically, the reference cases employ 25, 64, 36, 12, 100, and 6 boreholes for Riyadh, Jeddah, Dhahran, Tabuk, Jizan, and Turaif, respectively. The total borehole length is calculated by multiplying the number of boreholes by the depth of each individual borehole. The layout of the borehole field for each location is provided in Appendix A; however, land availability for the borehole grid was not considered in this study. Additional specifics regarding the borehole fields are presented in Table 1.

Table 3. Results of the GHE simulation in all cases.

	Description	Riyadh	Jeddah	Dhahran	Tabuk	Jizan	Turaif
Reference Cases	Number of boreholes	25	64	36	12	100	6
	Borehole depth (m)	80	80	80	80	80	80
	Total boreholes length (m)	2000	5120	2880	960	8000	480
	Total HP energy consumption (MWh)	1035	1302	1075	789	1453	650
CBRD Cases	Number of boreholes	16	28	20	8	36	4
	Borehole depth (m)	92	100	95	94	110	99
	Total boreholes length (m)	1472	2800	1900	752	3960	396
	Total HP energy consumption (MWh)	1020	1282	1062	785	1421	650
Savings	Savings in total borehole length	26%	45%	34%	22%	51%	18%
	Savings in total HP energy consumption	1.4%	1.6%	1.3%	0.5%	2.2%	0.0%

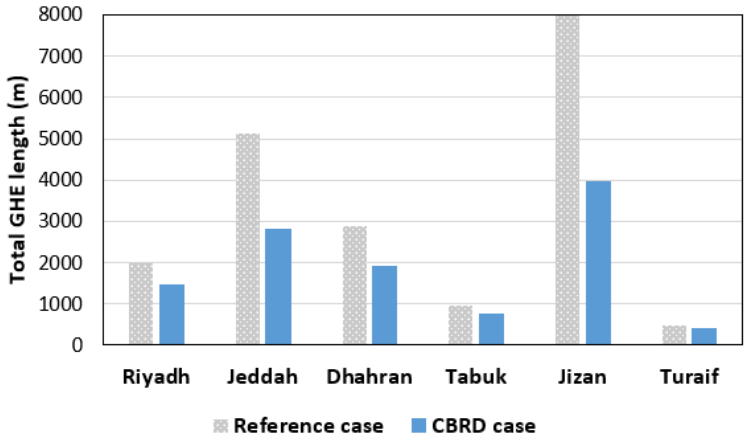


Figure 6. Total borehole length for the reference case and the CBRD case.

The g-function profiles, depicted in Figure 7, illustrate the thermal interaction between boreholes. The linear relationship observed at the early time (before $t/t_s \approx -4.5$) means that there is no thermal interaction between the boreholes across all locations. Given identical borehole spacing in all cases, initial thermal interaction primarily depends on site-specific thermal conductivity and dynamic building thermal loads. Thermal interaction is first observed in Jizan and Jeddah. Subsequent flips in the g-function profiles signify the initiation of heat transfer in both axial and radial directions. Finally, the g-function profiles tend towards a plateau, indicating the approach to a steady state. Turaif notably achieves a steady state after 30 years of operation, whereas other locations require additional time, attributed to the larger thermal storage volume in the ground.

Another anticipated result is the increase in the annual average outlet fluid temperature from the GHE over the 30-year operation period across all sites, as depicted in Figure 8. Note that the annual average outlet fluid temperature in some locations almost reaches a steady state. This is the annual average outlet fluid temperature, but the maximum outlet fluid temperatures are designed to reach 40 °C after 30 years of operation. A similar trend is observed in the heat pump energy consumption in all sites as illustrated in Figure 9. These increases in EFT and heat pump energy consumption are attributed to the significant imbalance between annual heating and cooling thermal loads, where the cooling peak load is at least twice the heating peak load.

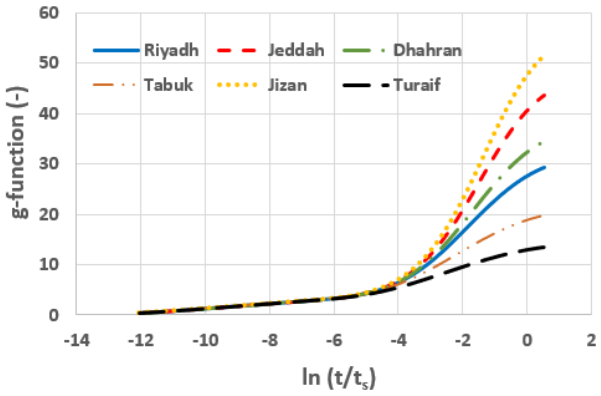


Figure 7. g-function of the reference cases.

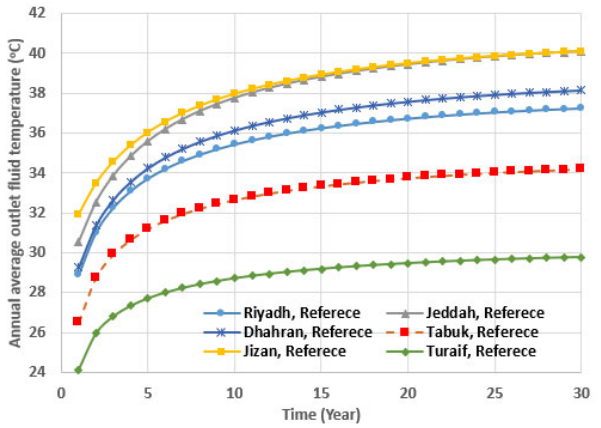


Figure 8. Annual average outlet fluid temperature from the GHE in reference cases.

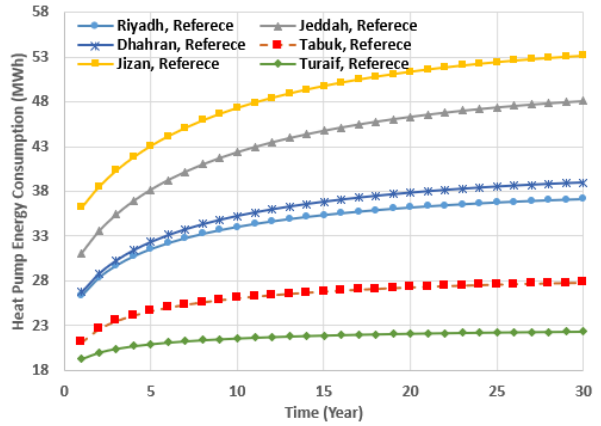


Figure 9. Annual heat pump energy consumption of the GHE in reference cases.

3.2. CBRD Cases

One expects, as explained in the literature review, that not all boreholes have the same efficiency and impact; therefore, a strategy of removing central boreholes (Figure 1) could potentially achieve comparable thermal performance while reducing the initial cost of the BHE system. Removing less effective boreholes may enable more consistent heat transfer throughout the bore field. The subsequent discussion examines the impact of completely removing boreholes from the central zone and increasing the depth of perimeter boreholes to achieve a maximum EFT of 40 °C while maintaining the current borehole spacing. The maximum borehole depth is not predetermined here and depends on practical constraints at the site.

The resulting number of boreholes for each site is shown in Table 3, and the total borehole lengths for the CBRD cases compared to the reference case are presented in Figure 6. The layout of the borehole field for each location is provided in Appendix A. Removing central boreholes increases the required depth of perimeter boreholes in all sites while reducing the total number of boreholes. The savings in total borehole length ranges from 18% to 51%, translating to substantial savings in the initial cost of the GSHP system. For instance, in Riyadh, the traditional 5 × 5 grid configuration (Figure 1a) requires 25 boreholes at a depth of 80 m. In contrast, when the central boreholes are removed (Figure 1b), only 16 perimeter boreholes are needed at a depth of 92 m, resulting in a 26% reduction in total borehole length. These savings are achieved without additional costs, highlighting the economic benefits of this design approach.

Achieving equivalent thermal performance with a significantly reduced size of the BHE system stems from mitigating thermal interaction between boreholes, thereby minimizing thermal build-up issues. This result is illustrated in Figure 10, where the thermal response factors (g-functions) are consistently lower in CBRD cases compared to the reference cases across all sites. The percentage reductions in g-functions correspond closely to the reductions in total borehole lengths. For example, in Riyadh, the g-function reaches 29 in the reference case but decreases to approximately 20 in the CBRD case.

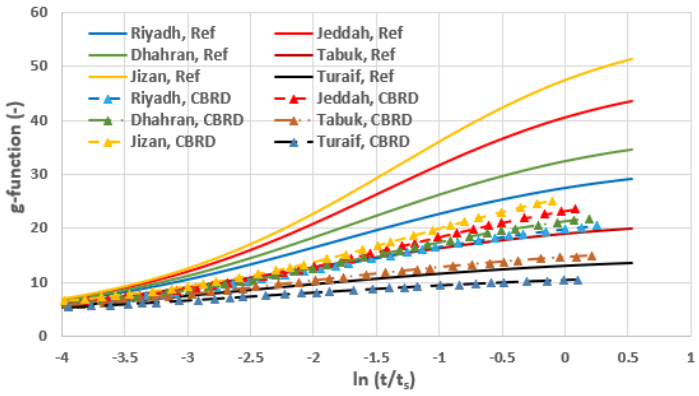


Figure 10. Comparison of g-function at the reference cases and CBRD cases.

Accordingly, the annual average outlet fluid temperatures from the GHE in the CBRD cases compared to the reference cases are shown in Figures 11 and 12. In the initial years, the annual average outlet fluid temperature from the GHE in the reference cases is lower (favorable for cooling-dominated buildings) than in the CBRD cases. However, over time, the EFT in the CBRD cases becomes lower. This occurs because the adverse effects of borehole thermal interactions are minimal at the beginning, allowing the GHE system to benefit from the larger number of boreholes. Yet, as borehole thermal interactions increase, the performance of the central boreholes decreases due to thermal build-up in the central zone. The total heat pump energy consumption over the 30 years of operation is shown in Table 3. The savings in total heat pump energy consumption over the 30 years range from 0% to 2.2%, which is insignificant compared to the substantial savings in the initial cost of the GSHP system. However, the long-term significance could evolve as building energy demands change over time due to several factors, such as shifts in building occupancy and usage patterns, and changes in buildings' energy efficiency which affect the heating and cooling needs. The goal of the CBRD approach is not primarily to save on total heat pump energy consumption but to address the significant barrier of high capital costs associated with GHE systems. Note that the energy savings do not account for the energy expenses related to marginal circulation pumping.

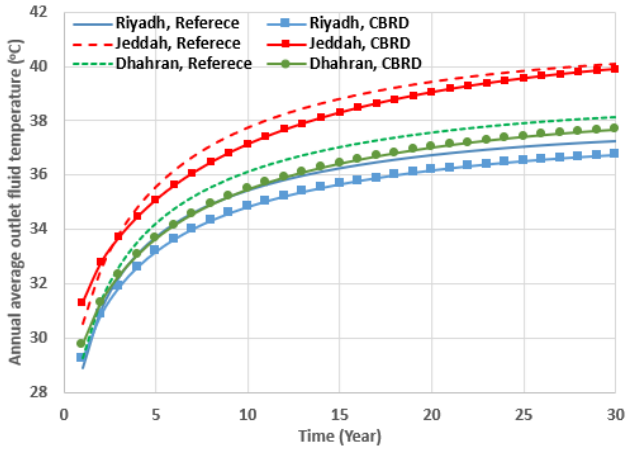


Figure 11. Comparison of annual average EFT for reference and CBRD cases.

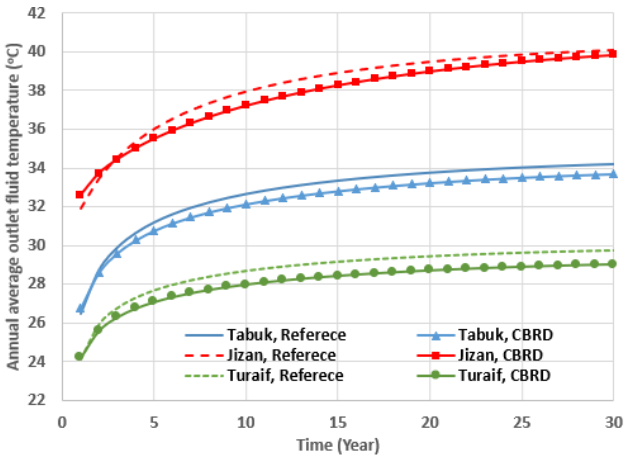


Figure 12. Comparison of annual average EFT for reference and CBRD cases.

3.3. Optimized CBRD Case

The previous results are not optimized, as optimization in this case requires detailed information about the available land area, drilling depth limits, number of boreholes, borehole spacings, and other factors. The optimization process used in this study involves minimizing the total borehole length while ensuring that the system operates within the desired thermal limits. The key objective is to maintain a maximum EFT, which serves as the primary constraint in all optimization cases. The algorithm starts with the removal of central boreholes in the CBRD approach, and further boreholes are removed in subsequent iterations to identify the optimal configuration. The optimization is constrained by several factors: the available land area for borehole placement, which limits the borehole spacings; drilling depth limits, set to a maximum of 150 m in this study to avoid excessively high drilling costs; and the need to maintain the system's thermal performance, particularly ensuring that the EFT does not exceed 40 °C under all conditions. The borehole depth is adjusted in each case to ensure that the system's thermal capacity remains sufficient, with deeper boreholes used when necessary to compensate for the reduced number of boreholes.

In this subsection, only the Riyadh location will be considered here as an example. The reference case of Riyadh (Figure 1a) will be used as a baseline, where the borehole depth is 80 m. The first case (called OP1) represents the CBRD scenario (Figure 1b), where all central boreholes are removed, resulting in a required borehole depth of 92 m and a total borehole length reduction of 26%. Further boreholes are removed in subsequent cases to find the optimal configuration. The layouts of these new cases are shown in Figure 13. The number

of boreholes for cases OP2, OP3, OP4, and OP5 is 12, 8, 6, and 5, respectively. The borehole depth and the savings in the total BHE length are presented in Figure 14. A 9% increase in borehole depth from OP1 (92 m) to OP2 (100 m) results in an increase in savings in the total BHE length from 26% to 40%. However, further removing boreholes with deeper boreholes does not lead to greater savings in the total BHE length. Therefore, although no optimized case has been identified for the Riyadh case, OP2 could be considered the best case because deeper boreholes increase the drilling cost without relatively significant savings in the total BHE length. The optimal case would be site-specific, as drilling costs are not always linear with depth due to varying ground layers at the same location. In this study, 150 m is chosen as the maximum allowable depth, with savings in the total BHE length reaching 62% in this scenario.

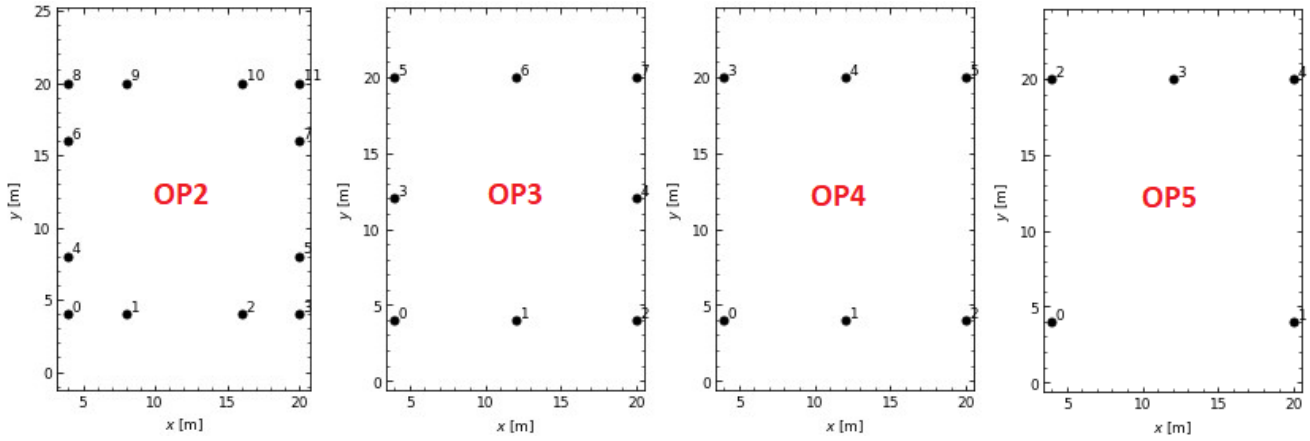


Figure 13. Layouts of the optimized cases from Riyadh case.

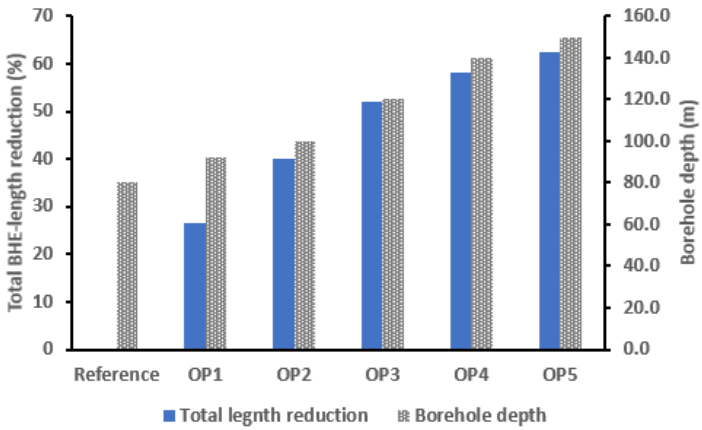


Figure 14. BHE-length reduction and borehole depth at optimization case.

Note that the effects of removing additional boreholes beyond the central ones could be explored in more detail. Potential trade-offs, such as the impact of ground thermal properties, available land area, and specific climate conditions, could influence the feasibility of further borehole removal while maintaining the desired system performance.

4. Conclusions

This study has explored the innovative design of removing central boreholes in vertical ground heat exchangers to enhance their thermal performance. By adapting the pygfunction Python package to design and simulate nontraditional borehole patterns under various building thermal loads and ground conditions, the impact of this design on system effi-

ciency and cost-effectiveness has been assessed. The following conclusions encapsulate the key insights and implications derived from this approach:

- Traditional design tools constrain borehole fields to rectangular grid patterns. The pygfunction Python package, however, allows for innovative borehole field patterns such as the central borehole removal design.
- In cooling-dominated buildings, thermal saturation tends to occur in the central zone of the borehole field, rendering the central boreholes less effective.
- The g-function profiles demonstrate a reduction in the interaction between boreholes in all CBRD cases, even with a reduction in the total BHE length.
- Compared to reference cases (traditional rectangular grid pattern), CBRD cases achieved up to a 51% reduction in total BHE length, resulting in significant savings in the initial cost of the GSHP system, without additional expenses.
- Over a 30-year period, the savings in total heat pump energy consumption were up to 2.2%, which, while modest, are overshadowed by the substantial initial cost savings.
- Additional reductions in total borehole length can be achieved by eliminating more boreholes beyond the central ones while maintaining a maximum EFT of 40 °C. Nevertheless, the optimized design will depend on factors such as available land area, drilling depth limits, number of boreholes, and borehole spacings.

Future research will focus on improving the pygfunction to optimize the tradeoff between borehole depth and the number of boreholes in the CBRD to achieve either the lowest life-cycle cost or minimize the initial cost of the system. Additionally, the CBRD could be explored by the use of subzones with separate geothermal heat pumps that remain off until specific conditions are met, potentially reducing operational costs and further enhancing the system's efficiency and economic viability.

Funding: This research was funded by the Deanship of Postgraduate Studies and Scientific Research at Majmaah University for funding this research work through project number (R-2025-1540).

Data Availability Statement: The original contributions presented in this study are included in the article.

Conflicts of Interest: The author declares no conflicts of interest.

Appendix A

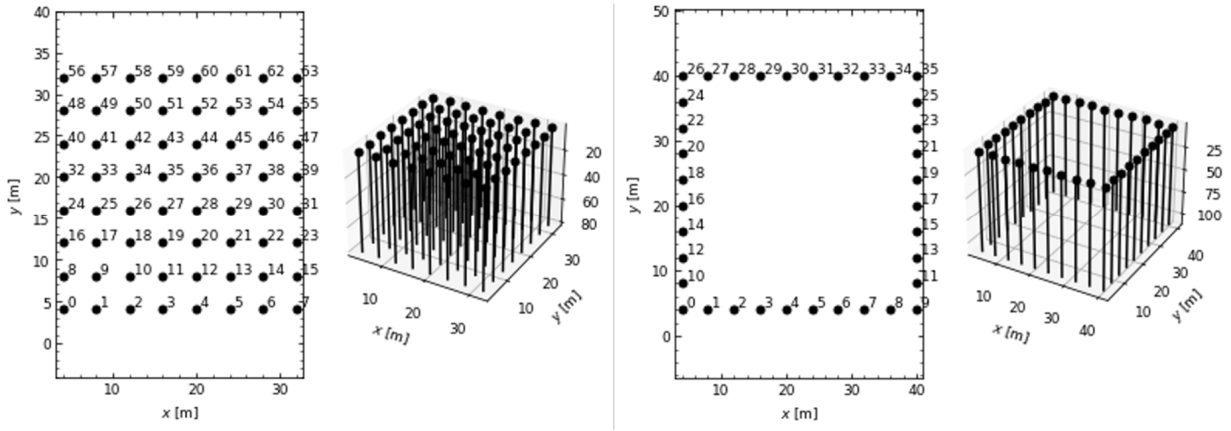


Figure A1. Bore field layout in Jeddah at traditional layout design and CBRD.

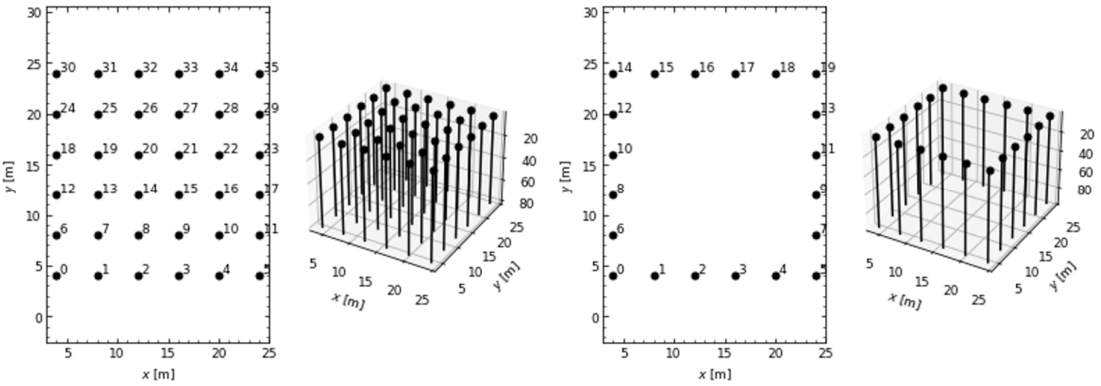


Figure A2. Bore field layout in Dhahran at traditional layout design and CBRD.

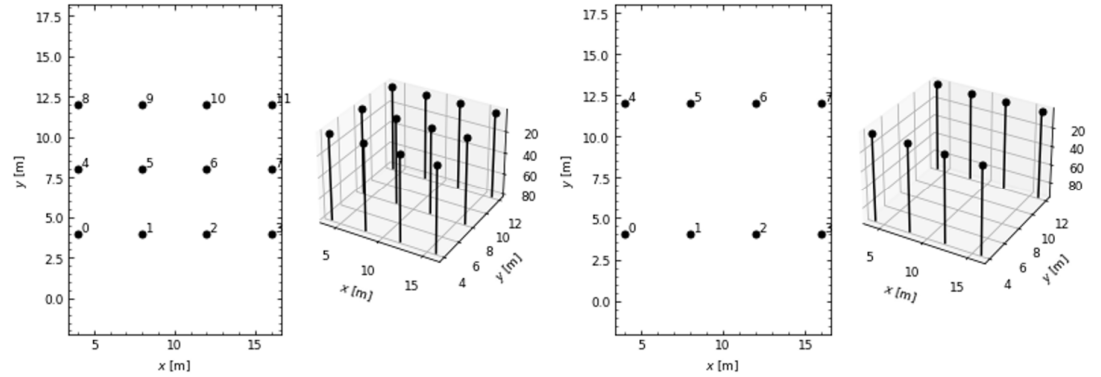


Figure A3. Bore field layout in Tabuk at traditional layout design and CBRD.

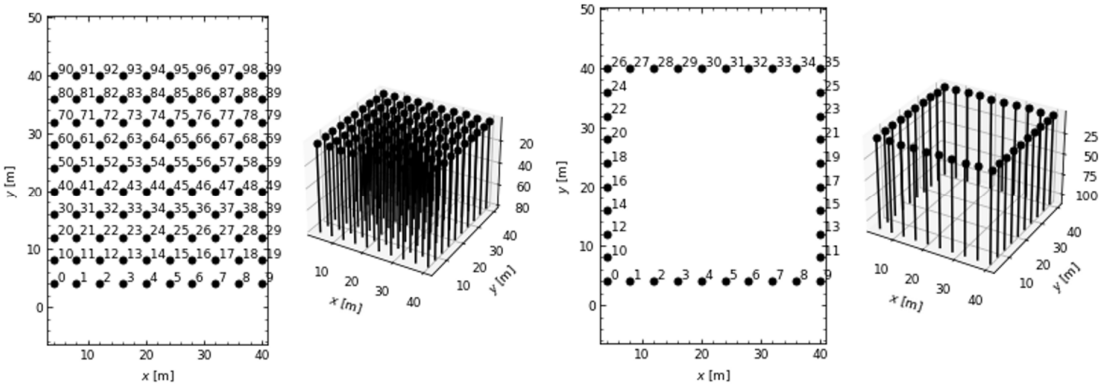


Figure A4. Bore field layout in Jizan at traditional layout design and CBRD.

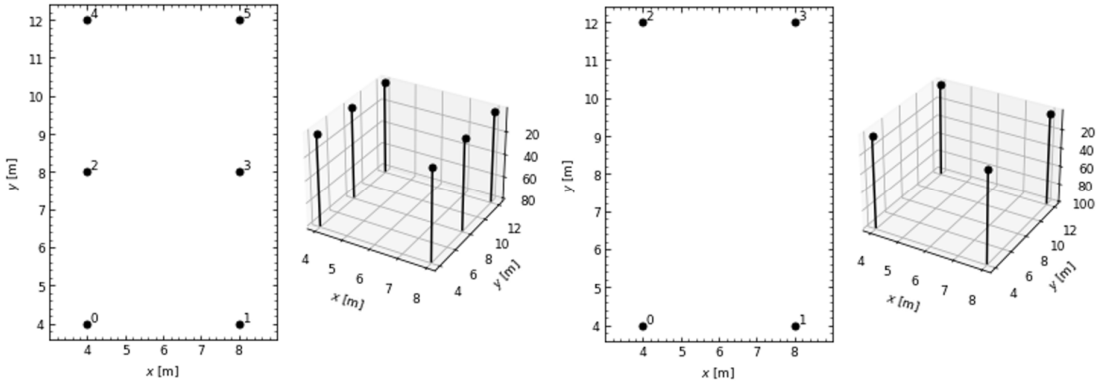


Figure A5. Bore field layout in Turaif at traditional layout design and CBRD.

References

1. Labus, K.; Labus, M.; Leśniak, G. Thermal properties of rocks from deep boreholes in Poland in terms of obtaining geothermal energy from enhanced geothermal systems. *Adv. Geo-Energy Res.* **2023**, *8*, 76–88. [CrossRef]
2. Zhuang, Y.; Huang, N.; Jiang, Y. Effect of Volumetric Flow Rate on Heat Transfer Characteristics of Single-Fractured Rock with Different Surface Morphology and External Temperature. *Processes* **2024**, *12*, 2821. [CrossRef]
3. Reichl, C.; Witte, H.J.L. Numerical Validation of a New Analytical Solution for Helical (Earth-Basket) Type Ground Heat Exchangers. *Processes* **2023**, *11*, 1418. [CrossRef]
4. Ishtiaque, M.-U.; Saha, P.; Sutradhar, A.; Galib, M.; Hannan, M.A. A sustainable approach to improve the efficiency of earth pipe cooling system. *Int. J. Sustain. Eng.* **2020**, *13*, 387–397. [CrossRef]
5. Alhajjaji, A.; Chiasson, A.; Aljabr, A. Simulation-Based Analysis of a Novel CO_2 Ground Source Heat Pipe (GSHP) to Reduce Temperature Fluctuations in Pavements in Different Climatic Conditions. *Energies* **2022**, *15*, 3343. [CrossRef]
6. Alnaqi, A.A.; Al-Rashed, A.A.A.A.; Alsarraf, J. Numerical investigation of the geometric parameters effect of helical blades installed on horizontal geo heat exchanger. *Geothermics* **2025**, *125*, 103169. [CrossRef]
7. Zhang, P.; Guo, B. Factors affecting the fluid temperature of geothermal energy wells converted from abandoned oil and gas wells. *Adv. Geo-Energy Res.* **2023**, *9*, 5–12. [CrossRef]
8. Gharbia, Y.; Derakhshandeh, J.F.; Amer, A.M.; Dinc, A. Geothermal Heat Pump for Space Cooling and Heating in Kuwaiti Climate. *Processes* **2024**, *12*, 910. [CrossRef]
9. Bae, S.; Nam, Y. Economic and environmental analysis of ground source heat pump system according to operation methods. *Geothermics* **2022**, *101*, 102373. [CrossRef]
10. Li, W.; Li, X.; Wang, Y.; Tu, J. An integrated predictive model of the long-term performance of ground source heat pump (GSHP) systems. *Energy Build.* **2018**, *159*, 309–318. [CrossRef]
11. Chen, F.; Mao, J.; Zhu, G.; Zhang, B.; Tian, Y.; Liao, D.; Liu, Y. Numerical assessment on the thermal imbalance of multiple ground heat exchangers connected in parallel. *Geothermics* **2021**, *96*, 102191. [CrossRef]
12. Wan, Y.; Yuan, Y.; Zhou, C.; Liu, L. Multiphysics coupling in exploitation and utilization of geo-energy: State-of-the-art and future perspectives. *Adv. Geo-Energy Res.* **2023**, *10*, 7–13. [CrossRef]
13. Mehrjerdi, A.K.; Åkesson, D.; Skrifvars, M. Influence of talc fillers on bimodal polyethylene composites for ground heat exchangers. *J. Appl. Polym. Sci.* **2020**, *137*, 49290. [CrossRef]
14. Wang, F.; You, T. Comparative analysis on the life cycle climate performance of ground source heat pump using alternative refrigerants. *Case Stud. Therm. Eng.* **2023**, *42*, 102761. [CrossRef]
15. Aljabr, A.; Chiasson, A.; Alhajjaji, A. Numerical Modeling of The Effects of Micro-Encapsulated Phase Change Materials Intermixed with Grout in Vertical Borehole Heat Exchangers. *Geothermics* **2021**, *96*, 102–197. [CrossRef]
16. Ballerini, V.; di Schio, E.R.; Valdiserri, P.; Naldi, C.; Dongellini, M. A Long-Term Dynamic Analysis of Heat Pumps Coupled to Ground Heated by Solar Collectors. *Appl. Sci.* **2023**, *13*, 7651. [CrossRef]
17. You, T.; Shi, W.; Wang, B.; Wu, W.; Li, X. A new ground-coupled heat pump system integrated with a multi-mode air-source heat compensator to eliminate thermal imbalance in cold regions. *Energy Build.* **2015**, *107*, 103–112. [CrossRef]
18. You, T.; Wang, B.; Wu, W.; Shi, W.; Li, X. A new solution for underground thermal imbalance of ground- coupled heat pump systems in cold regions: Heat compensation unit with thermosyphon. *Appl. Therm. Eng.* **2014**, *64*, 283–292. [CrossRef]
19. Aljabr, A.; Chiasson, A. Numerical modeling of the effects of the radial and axial location of added micro-encapsulated phase change materials in vertical borehole heat exchangers. *Geothermics* **2023**, *110*, 102684. [CrossRef]
20. Liu, X.; Spitler, J.D.; Qu, M.; Shi, L. Recent developments in the design of vertical borehole ground heat exchangers for cost reduction and thermal energy storage. *J. Energy Resour. Technol. Trans. ASME* **2021**, *143*, 1–13. [CrossRef]
21. Spitler, J.; Cook, J.; Liu, X. Recent experiences calculating g-functions for use in simulation of ground heat exchangers. *Trans. Geotherm. Resour. Counc.* **2020**, *44*, 296–315.
22. Eskilson, P. Thermal Analysis of Heat Extraction Boreholes. Ph.D. Thesis, University of Lund, Lund, Sweden, 1987.
23. Chiasson, A.D. *Geothermal Heat Pump and Heat Engine Systems: Theory and Practice*, 1st ed.; Wiley: Hoboken, NJ, USA, 2016.
24. Cimmino, M. pygfunction: An open-source toolbox for the evaluation of thermal response factors for geothermal borehole fields. In Proceedings of the eSim 2018, the 10th Conference of IBPSA-Canada, Montréal, QC, Canada, 9–10 May 2018; pp. 492–501.
25. Cimmino, M.; Bernier, M. A semi-analytical method to generate g-functions for geothermal bore fields. *Int. J. Heat Mass Transf.* **2014**, *70*, 641–650. [CrossRef]
26. Cimmino, M. Semi-Analytical Method for g-function Calculation of bore fields with series- and parallel-connected boreholes. *Sci. Technol. Built Environ.* **2019**, *25*, 1007–1022. [CrossRef]
27. Alkhwildi, A. *Thermal Energy Storage in Geothermal Heat Pump Systems*; University of Dayton: Dayton, OH, USA, 2021.
28. Bayer, P.; de Paly, M.; Beck, M. Strategic optimization of borehole heat exchanger field for seasonal geothermal heating and cooling. *Appl. Energy* **2014**, *136*, 445–453. [CrossRef]

29. Spitler, J.D.; Cook, J.C.; Liu, X. A Preliminary Investigation on the Cost Reduction Potential of Optimizing Bore Fields for Commercial Ground Source Heat Pump Systems. In Proceedings of the 45th Workshop on Geothermal Reservoir Engineering, Stanford, CA, USA, 10–12 February 2020; pp. 1–13.
30. Aljabr, A. Investigation on the influence of mixed borehole depths in vertical ground heat exchanger systems. *Geothermics* **2024**, *119*, 102971. [CrossRef]
31. Cimmino, M.; Cook, J.C. pygfunction 2.2: New features and improvements in accuracy and computational efficiency. In Proceedings of the IGSHPA Research Track 2022, International Ground Source Heat Pump Association, Las Vegas, NV, USA, 6–8 December 2022; pp. 45–52.
32. Claesson, J.; Hellström, G. Multipole method to calculate borehole thermal resistances in a borehole heat exchanger. *HVACR Res.* **2011**, *17*, 895–911. [CrossRef]
33. Claesson, J.; Javed, S. A load-aggregation method to calculate extraction temperatures of borehole heat exchangers. In *ASHRAE Transactions (118, Issue 1)*; American Society of Heating, Refrigerating, and Air-Conditioning Engineers, Inc. (ASHRAE): Atlanta, GA, USA, 2012.
34. Aljabr, A.; Almoatham, S. The potential of utilizing vertical borehole heat exchangers in residential buildings for the various climate zones of Saudi Arabia. *Geothermics* **2024**, *122*, 103087. [CrossRef]
35. Krarti, M.; Aldubyan, M.; Williams, E. Residential building stock model for evaluating energy retrofit programs in Saudi Arabia. *Energy* **2020**, *195*, 116980. [CrossRef]
36. Ayadi, B.; Al-Ebrahim, M.A.; Rajhi, W.; Abu-Hamdeh, N.H.; Nusier, O.K.; Pham, V.; Karimipour, A. Simultaneous use of renewable energies and phase change materials to reduce energy consumption in Saudi buildings: Examine the photovoltaic cells. *Case Stud. Therm. Eng.* **2024**, *55*, 104143. [CrossRef]
37. Hakky, R.I. Garden of the Saudi Villa: Its Drawbacks and Prospects. *J. Archit. Plan.* **2013**, *25*, 51–68.

Disclaimer/Publisher's Note: The statements, opinions and data contained in all publications are solely those of the individual author(s) and contributor(s) and not of MDPI and/or the editor(s). MDPI and/or the editor(s) disclaim responsibility for any injury to people or property resulting from any ideas, methods, instructions or products referred to in the content.